Journal of
Alzheimer's Disease & Parkinsonism

Dazortsava et al., J Alzheimers Dis Parkinsonism 2018, 8:6
DOI: 10.4172/2161-0460.1000454

Research Article Open Access

Implication of GPR40 Signaling in the Subventricular Zone Neurogenesis after Ischemia *via* Cross-Talk between Neural Progenitors and Microglia

Maryia Y Dazortsava[1,3]*, Ilya V Pyko[2], Nadezhda B Boneva[3], Anton B Tonchev[3,4], Zhu H[3], Sawamoto K[5], Minabe Y[1] and Yamashima T[1,3]

[1]*Department of Psychiatry and Behavioral Science, Division of Neuroscience, Graduate School of Medical Science, Kanazawa University, 13-1 Takara-machi, 920-8640, Kanazawa, Ishikawa, Japan*
[2]*Division of Translational and Clinical Oncology, Cancer Research Institute, Kanazawa University, 13-1 Takara-machi, 920-0934, Kanazawa, Ishikawa, Japan*
[3]*Department of Restorative Neurosurgery, Division of Neuroscience, Graduate School of Medical Science, Kanazawa University, 13-1 Takara-machi, 920-8641, Kanazawa, Ishikawa, Japan*
[4]*Department of Anatomy, Histology and Embryology, Medical University-Varna, Marin Drinov str. 55, 9002 Varna, Bulgaria*
[5]*Department of Developmental and Regenerative Biology, Institute of Molecular Medicine, Graduate School of Medical Sciences, Nagoya City University, 1-Kawasumi, Mizuho-cho, Mizuho-ku, Nagoya 467-8601, Japan*

Abstract

Objective: Sub-ventricular Zone (SVZ) of the anterior horn of lateral ventricle is a source of neural stem cells in the adult mammalian brain along with hippocampal Sub-granular Zone (SGZ). Previously, we demonstrated that transient global brain ischemia in adult monkeys increases the number of neuronal progenitors in the SGZ *via* G-protein-coupled Receptor 40 (GPR40) signaling. Sonic Hedgehog (SHH) is indispensable for ischemia-induced neural progenitor proliferation in rodents. Although GPR40 is expressed in the SVZ, GPR40 synergy with SHH remains unelucidated in adult SVZ neurogenesis. Here, we studied GPR40 implication in SVZ neurogenesis using monkey model.

Methods: Adult monkeys underwent 20 min transient global brain ischemia by clamping both the innominate and left subclavian arteries. On days 3, 4, 7, 9 and 15 after ischemia/reperfusion, when SVZ neurogenesis increases, as it was shown previously by the authors, the brain samples were resected and normal and post-ischemic monkey SVZ tissues were used for Western blot and immunofluorescence histochemistry analysis.

Results: Ischemia/reperfusion increased GPR40 protein levels, proliferation of GPR40-positive stem/progenitor cells, the number of GPR40/PSA-NCAM or GPR40/doublecortin co-expressing immature neurons and GPR40-positive microglial cells in the SVZ vascular niche. GPR40 up-regulation correlated with that of SHH, Notch1 and β1-integrin; GPR40 co-localized with stem/progenitor cell markers in post-ischemic SVZ. GPR40-positive microglia showed the highest SHH expression relative to other cell types. SHH binding to Patched1 in the cells that surrounded GPR40/SHH-expressing microglia occurred within the distance of SHH paracrine secretion.

Conclusion: These data suggest that GPR40 is related to post-ischemic neurogenesis in the primate SVZ, GPR40-positive microglia support SHH paracrine secretion in the SVZ, and the cross-talk between perivasucular microglia and neuronal progenitors may be crucial in the vascular niche to activate neurogenesis by SHH and Notch1 signaling.

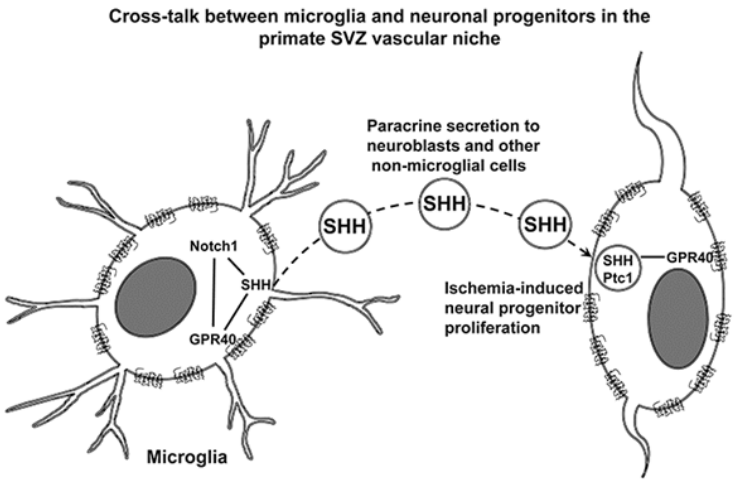

***Corresponding author:** Maryia Y Dazortsava, Department of Psychiatry and Behavioral Science, Division of Neuroscience, Graduate School of Medical Science, Kanazawa University, 13-1 Takara-machi, 920-8640, Kanazawa, Ishikawa, Japan, Tel: +81 76 265 2307; E-mail: maria1108@gmail.com

Received: November 15, 2018; **Accepted:** November 17, 2018; **Published:** November 24, 2018

Citation: Dazortsava MY, Pyko IV, Boneva NB, Tonchev AB, Zhu H, et al. (2018) Implication of GPR40 Signaling in the Subventricular Zone Neurogenesis after Ischemia *via* Cross-Talk between Neural Progenitors and Microglia. J Alzheimers Dis Parkinsonism 8: 454. doi: 10.4172/2161-0460.1000454

Keywords: GPR40; Cerebral ischemia; Adult monkey neurogenesis; Sonic hedgehog; Notch1; Sox2

Abbreviations: BrdU: 5-bromo-2-deoxyuridine; CNS: Central Nervous System; GPR40: G-protein-Coupled Receptor 40; NSCs: Neural Stem Cells; Ptc1: Patched1; SGZ: Sub-granular Zone of the Hippocampal Dentate Gyrus; SHH: Sonic Hedgehog; SVZ: Sub-ventricular Zone of the Anterior Horn of Lateral Ventricle; TGBI: Transient Global Brain Ischemia

Introduction

Most of the neurons in the Central Nervous System (CNS) are produced during embryonic development, which was thought for long years to be the only source of adult neurons. However, this dogma was challenged by the discovery of neurogenesis in adult mammalians [1]. Thereafter, it was demonstrated that the adult human brain is capable for neuronal production [2] and migration of Neural Stem Cells (NSCs) [3] which is required for learning [4] and memory [5]. Currently, two regions in adult mammalians are known to be involved in neurogenesis: the hippocampus and the subventricular zone along the walls of the lateral ventricle [6]. Since the subventricular zone is an active neurogenic niche [2,7,8], a subpopulation of astrocytes with stem cell features resides within the subventricular zone in mammalians [9] including monkeys [10,11] and humans [8].

Sub-ventricular zone is located in the lateral walls of the lateral ventricle, consisting of four distinct cellular layers in humans and monkeys. The layer lining the lateral ventricles (Layer I) is a monolayer of ependymal cells with basal expansions that are interconnected with astrocytic processes in the hypocellular layer (Layer II). Layer II, is largely devoid of cell bodies except for rare astrocytes and neuronal somata [7]. It is suggested that the astrocytic and ependymal interconnections in Layer II may control stem cell proliferation and differentiation. A ribbon of astrocyte cell bodies (Layer III) is adjacent to Layer II. Subpopulation of astrocytes within the Layer III represents a pool of multipotent progenitor/stem cells. Layer IV, is a transition region to the underlying brain parenchyma characterized by the presence of myelin [7,8]. Subventricular zone in the anterior horn of the cerebral lateral ventricle (abbreviated as SVZ in this paper) of adult mammals contains multipotent progenitor/stem cells, which are supposedly maintained in the vascular niche. SVZ is extensively vascularized by a rich plexus of blood vessels [12,13]. Moreover, neural progenitors in the SVZ contact with blood vessels at sites devoid of the blood brain barrier [13]. We have previously shown that neuronal progenitor cells may derive from adventitial cells of arterioles in primate brain [14].

SVZ contains a microenvironment of interacting cells and extracellular molecules that promote neurogenesis [15,16]. Microglia is present in the vascular niche of SVZ and directly interact with NSCs to enhance neurogenesis [16,17] and oligodendrogenesis in SVZ [18]. It has been shown that microglia eliminate unnecessary cells, axons and synapses in SVZ [19]. On the other hand, neural progenitors regulate microglia, proliferation, migration, and phagocytosis *via* the secretion of immunomodulatory proteins [20]. Cerebral ischemia enhances the proliferation of neural progenitor cells in adult rodent SVZ [21]. We have previously reported that the proliferation of progenitor cells in monkey SVZ increases after Transient Global Brain Ischemia (TGBI) with subsequent migration of a part of the progenitors to the rostral migratory stream, and that ischemia increases the proportion of adult–generated neural precursors retaining their location in SVZ for months after injury [11].

GPR40 (also called FFAR1) is a member of the subfamily of homologous G-protein-coupled receptors with seven-transmembrane domains [22]. GRP40 is a non-specific receptor for medium- and long-chain Poly-unsaturated Fatty Acids (PUFA) including docosahexaenoic and arachidonic acids, and their binding to GPR40 initiates an intracellular signalling *via* phospholipase C and phosphatidylinositol turnover [23,24]. GPR40 is predominantly expressed in the brain and pancreas in primates [24]. GPR40 regulates insulin secretion in the pancreas [23]. In humans and monkeys, GPR40 is expressed in the neurons and astrocytes throughout the brain including the SVZ and the subgranular zone of the hippocampal dentate gyrus [24,25]. GPR40 activation protects from neuronal inflammation and insulin resistance [26]. GPR40 is thought to be closely related to the brain development, adult neurogenesis, learning and memory [27-29]. We found that GPR40 is expressed in the CNS of adult monkeys especially in neural progenitors, new born neurons and astrocytes after TGBI in the hippocampal neurogenic niche [28,30]. We also reported that GPR40 is up-regulated by PUFA in the monkey hippocampus after TGBI and induces phosphorylation of CREB [31,32]. Moreover, one of the GPR40 ligands, docosahexaenoic acid can prevent brain damage by ischemia [33].

Sonic Hedgehog (SHH) is a signaling molecule, which regulates ischemia-induced neural progenitor proliferation [34]. SHH signaling involves it

a) paracrine secretion by SHH producing cells,

b) transport over considerable distances,

c) consequent binding to Patched1 (Ptc1) receptors on the surface of SHH responding cells and internalization of Ptc1/SHH complexes into endosomes [35] and

d) their targeting for protein degradation [36] with half-life less than 1 h [37].

Pathways of GPR40 signaling in the primate SVZ neurogenic niche and its effects on SVZ neurogenesis *in vivo* are not clearly known. Here, we studied the implication of GPR40 signaling in ischemia-enhanced neurogenesis in the adult monkey SVZ. The purpose is to determine if the changes in expression of the GPR40 after TGBI are associated with activation of neurogenesis in SVZ as demonstrated in the hippocampal neurogenic niche of postischemic monkeys [30]. The results suggest that GPR40 expression is involved in the neurogenic differentiation of stem/progenitor cells in the adult monkey SVZ and that perivascular GPR40 expression is implicated in post-ischemic neurogenesis in adult monkeys in the SVZ neurogenic niche. The cross-talk between perivascular microglia and neuronal progenitors is crucial in the vascular niche to activate neurogenesis by SHH and Notch1 signaling.

Materials and Methods

Animal procedures for the model of ischemia-enhanced adult neurogenesis

Animal experiments were done at the Institute for Experimental Animals, Kanazawa University Advanced Science Research Center. Surgical procedures and postoperative care of animals were done in accordance with the guidelines of the Animal Care and Ethics Committee of Kanazawa University and the NIH Guide for Care and Use of Laboratory Animals and with efforts made to minimize the number of animals used and their suffering. Young adult Japanese monkeys (*Macaca fuscata*) were bred in air-conditioned cages and allowed to have free daily access to food and water. For TGBI experiments the total

number of 5-10 years old animals (27 monkeys) was divided into five experimental groups of monkeys for Western blotting (15 monkeys, n=3 for each group of the control and post-ischemic days 3,7,9,15), and four experimental groups for immunofluorescence histochemical analyses (12 monkeys, n=3 for each group of the control and post-ischemic days 4,9,15). TGBI was made under general anesthesia, by clamping the innominate and left subclavian arteries for 20 min, according to the procedure described previously [38,39], whereas the control monkeys underwent a sham-operation. To label newly generated cells in adult macaque monkeys 5-bromo-2-deoxyuridine (BrdU) (Sigma, St Louis, MO) was intravenously injected in the saphenous vein at a dose of 100 mg/kg for five consecutive days before euthanasia. Monkeys were sacrificed after the operation in respective groups on days 4, 7, 9 and 15 for the brain tissue sampling.

Immunofluorescent Microscopy

For the immunofluorescence analysis, monkeys were perfused with 0.5 L of ice-cold saline followed by 1 L of 4% Paraformaldehyde (PFA) from the left ventricle. The brain was removed and the SVZ tissue samples were resected and post-fixed in 4% PFA for 48 h. The samples were cryoprotected in 30% sucrose followed by embedding in OCT (Optimal Cutting Temperature) compound (Tissue-Tek, Sakura Finetech, Tokyo, Japan). The frozen samples were cut into 40-µm sections on a Leica CM3050 cryomicrotome (Leica, Wetzlar, Germany). The sections were stored in a cryopreservation buffer containing 25% ethylene glycol and 25% glycerol in 0.05 M phosphate buffer at -20˚C until the sections were stained.

To reveal incorporated BrdU, BrdU staining was preceded by DNA denaturation in free-floating sections by incubation in 50% formamide/50% 2×SSC buffer (0.3 M NaCl, 0.03 M sodium citrate) for 2 h at 65ºC, followed by 30 min incubation in 2N HCl at 37ºC, as described previously [40].

The SVZ free-floating sections were washed in the Phosphate-buffered Saline (PBS) and permeabilized with 0.1% Triton X-100/ Digitonin 500 µg/mL for 20 min at room temperature. To block non-specific bindings, the sections were incubated for 1 h at room temperature with 5% goat (Vector Laboratories, Burlingame, CA) or 5% donkey serum (Sigma), 1% bovine serum albumin, 0.1% Triton X-100/ Digitonin 500 µg/mL in PBS. Incubation with primary antibodies (Table 1) was done with 0.1% Triton X-100/Digiton 500 µg/mL in 5% goat/donkey serum and 1% glycerin at 4˚C for 48 h. Respective anti-rabbit or anti-mouse secondary antibodies of goat or donkey origin conjugated to Alexa Fluor-488, -546 or -633 (Invitrogen, Grand Island, NY) were used at 1:200 dilution with overnight incubation at 4˚C in the dark. Negative controls were made by omitting the respective primary antibody. The stained sections were mounted on the glass slides by using Vectashield mounting medium (Vector Laboratories). Digital images were obtained using a confocal laser scanning microscope (LSM 510; Carl Zeiss, Oberkochen, Germany) and relative fluorescence intensities were analyzed by using Zen 2009 software (Carl Zeiss).

BrdU-positive cells were evaluated on series of every 12th section through the region of interest, as described previously [11]. Vessels stained with 4',6-diamidino-2-phenylindole (DAPI) or other markers were detected on X-Y plane: lumen images were taken in the X-Y plane by focusing in the middle of the vessel, a group of five images of different high-power full microscopic fields were captured along the vessel. Vascular wall and perivascular space morphology was determined in the Z axis from stacks of serial images (1.5 µm thick) by the differences in shape and orientation of the cells and their nuclei in vascular wall layers, as described previously [41].

Target of the antibody		Manufacturer, catalog number (cat.#)	Host Species	Type	IF Dilution	WB Dilution
GPR40	G protein-coupled receptor40; Free fatty acid receptor 1 (FFA1 ,FFAR1)	Peptide; # AD-807-AK1	Rabbit	IgG	1:50	1:2500
BrdU	5-bromo-2-deoxyuridine	Abcam; #ab6326	Rat	Monoclonal IgG_{2a}	1:100	
		Harlan Sara-Lab	Rat		1:100	
GFAP	Glial Fibrillary Acidic Protein	Millipore; #MAB3402	Mouse	Monoclonal IgG_1	1:500	
PSA-NCAM	Polysialylated-neural cell adhesion molecule	A gift from Dr. Tetsunori Seki	Mouse	IgM	1:400	
CD31	Platelet/endothelial cell adhesion molecule (PECAM-1)	Dako; #IR610	Mouse	Monoclonal IgG_1	1:50	
		Termo scientific; #RB-10333	Rabbit	Polyclonal	1:50	
Ng2	Neural/glial antigen 2	Novosbio; NB100-2688AF405	Mouse	Monoclonal	1:50	
Iba1	Ionized calcium-binding adapter molecule 1; Allograft inflammatory factor 1 (AIF-1)	A gift from Dr.Yoshinori Imai	Rabbit	Monoclonal	1:700	
Dcx	Double cortin	Santa Cruz; #sc-8066	Goat	Polyclonal IgG	1:200	
SHH	Sonic Hedgehog	Santa Cruz; #sc-373779	Mouse	Monoclonal IgG_1	1:100	1:1000
Notch1	Notch homolog 1	Santa Cruz; #sc-6014	Goat	Polyclonal	1:50	
		Abcam; #ab27526	Rabbit	Polyclonal		1:300
Sox2	Sex determining region Y-box	Millipore; #ab5603; #ab5770	Rabbit	Polyclonal	1:100	1:5000
Ptc1	Patched 1	Santa Cruz; #sc-6147	Goat	Polyclonal IgG	1:50	
FABP7	Fatty-acid-binding protein 7 ; Fatty-acid-binding protein brain type (B-FABP)	R&D Systems; #AF3166	Goat	Polyclonal IgG	1:50	
CD29	Integrin b-1	Abcam; #ab52971	Rabbit	Monoclonal IgG		1:2500
		Termo scientific; #MS-596	Mouse	Monoclonal IgG_1	1:100	

Table 1: List of primary antibodies utilized in the Western blot and immunofluorescent microscopy analyses.

For the quantification of obtained microscopy data the mean number of cells double-positive for respective expression markers in five high-power full microscopic fields was calculated with standard deviations. Quantitative analysis for immunoreactivity colocalization between GPR40 and SHH was performed with the Fiji image processing package by using the colocalization measurement function of the JaCoP plugin [42]. The colocalization index is represented by Pearson's coefficient calculated following Costes randomization and unbiased automatic threshold calculation [43]. Colocalization index values within intervals 0-0.49; 0.50-0.70; 0.71-0.88; 0.89-0.97; 0.98-1.0 reveal very weak, weak, moderate, strong and very strong colocalization, respectively [44].

Western blot analysis

For the Western blot analysis, animals of the control and post-ischemic days 3,7,9 and 15 experimental groups were quickly perfused with ice-cold saline. The brain was removed and cut into small samples, immediately frozen in liquid nitrogen and stocked at -80˚C. For the total protein extraction, the samples were lysed in Radio Immunoprecipitation Assay buffer (Sigma) supplemented with protease and phosphatase inhibitor cocktails (Sigma). The lysates were sonicated and centrifuged at 15,000 g and the supernatant was collected. Protein concentrations were determined using the bicinchoninic acid assay procedure (Pierce Biotechnology, Rockford, IL), with bovine serum albumin as a standard. Equivalent amounts of the whole tissue lysate protein (15 μg) were separated by gel electrophoresis and transferred to polyvinylidene difluoride membrane (Invitrogen) by electroblotting, according to the standard procedure as described in the manufacturer's protocol. The polyvinylidene difluoride membrane was blocked with 5% skim milk in Tris-buffered saline, pH 8.0, with 0.1% Tween-20 before addition of primary antibody. Membranes were washed and incubated with horseradish peroxidase-conjugated secondary antibody. Detection was done by using a Pierce ECL Plus Western Blotting Substrate, (Thermo Fisher scientific, Rockford, IL), and compact luminescent image analysis system (Fujifilm, LAS-4000mini) with LAS-4000mini Image Reader software v.2.0. Densitometric analysis was done using image processing software (NIH, ImageJ, 1.48i). The source and working dilutions of the primary antibodies are listed in Table 1. β-actin was used as loading control.

Statistical Analyses

Statistical analyses were done using Mann–Whitney U-test, Kruskal-Wallis one-way ANOVA test, Pearson product-moment correlation coefficient and linear regression analysis. $P<0.05$ was considered significant.

Results

Overall expression of GPR40 in SVZ after ischemia

We first studied GPR40 expression in the SVZ of adult monkeys under normal condition and after TGBI by Western blot and immunofluorescence. Western blot analysis showed a significant increase of GPR40 protein levels in SVZ starting from day 3 after ischemia with the maximum on days 9 and 15 in comparison to the sham-operated control (Figure 1A). Laser confocal microscopy showed an increase of perivascular expression of GPR40 on days 9 and 15 in the gap layer in comparison to the control. Area of high GPR40 expression has extended beyond the gap layer of SVZ zone on day 9 (Figure 1B). GPR40+ cells were accumulated in close vicinity to vessels in the SVZ on day 15 after ischemia (Figure 1C).

Expression of GPR40 by proliferating cells in SVZ after ischemia

To confirm the role of GPR40 expression for neurogenesis in the monkey SVZ after ischemia the relation of GPR40 to newly generated cells, labelled with BrdU was studied by immunofluorescence. The number of BrdU-positive progenitor cells increased after ischemia (Figure 1B) and these cells were frequently seen near blood vessels. Laser confocal microscopy showed that GPR40 expression was found in the majority of BrdU-positive newly generated cells in the SVZ (Figure 1D). A significant increase of the expression of GPR40 was seen in BrdU-positive cells on days 9 and 15 after ischemia (Figures 1D and E). This is consistent with our previous data demonstrating maximal proliferation of progenitor cells in SVZ [11] and maximal expression of GPR40 in the monkey hippocampus [30] on the second week after ischemia. Moreover, the observed increase of GPR40 expression by BrdU-positive cells was often seen in the vascular niche in SVZ (Figure 1B).

Expression of GPR40 by neural stem/progenitor cells in SVZ after ischemia

To estimate the post-ischemic expression of GPR40 in the proliferating astrocytes known to represent NSCs in primate SVZ ribbon [8] the expression of GPR40 in cells positive for GFAP and BrdU, was studied by immunofluorescence (Figure 2A). On day 9 after ischemia only few of BrdU-positive cells near vessels were GFAP-positive (Figure 2A). Many of $BrdU^+/GFAP^+$ cells were also positive for GPR40 (Figure 2A) while $BrdU^+/GFAP^+$ cells were hardly detectable in the non-ischemic controls (Figure 2A). On the other hand, we found many cells with GPR40+/GFAP+/BrdU- phenotype near vessels in the gap layer (Figure 2A) as well as GPR40+/GFAP-/BrdU+ phenotype (Figure 2A) or GPR40-/GFAP-/BrdU+ phenotype (Figure 2A) both in control and after ischemia.

To further assess implication of GPR40 for the neurogenic differentiation of SVZ neuronal progenitors, the co-staining of the GPR40 was done using antibody against double cortin (Dcx) a marker for migrating immature neurons retained in neurogenic areas in the adult SVZ [45]. Immunofluorescence microscopic analysis of GPR40 expression in Dcx-positive immature neurons showed an increase of the number of GPR40/Dcx co-expressing cells in the SVZ on days 9 and 15 after ischemia (Figure 2B). GPR40/Dcx co-expressing immature neurons were mainly located in the SVZ gap layer (Figure 2B). Moreover, the incidence of Dcx-positive cells among GPR40-expressing cells significantly increased on days 9 and 15 after ischemia (Figure 2C). Polysialylated neural cell adhesion molecule (PSA-NCAM) is an another marker for adult neurogenesis which is expressed in immature neurons [46]. The immunoreactivity of GPR40 in PSA-NCAM-positive immature neurons was estimated in the monkey SVZ of the control, day 9 and 15 after ischemia. The immunofluorescence data showed that PSA-NCAM expression considerably increased on days 9 and 15 after ischemia (Figure 2D). The number of GPR40/PSA-NCAM co-expressing cells increased in the SVZ vascular niche on days 9 and 15 after ischemia (Figure 2D). Polysialylated-neural Cell Adhesion Molecule (PSA-NCAM) expression was seen in the gap layer especially in the cells close to the vessels (Figure 2D). That was concomitant with the increase of GPR40 expression in perivascular cells on day 9 after ischemia (Figure 1B).These data suggest that GPR40 up-regulation may be implicated for the neuronal differentiation of multipotent

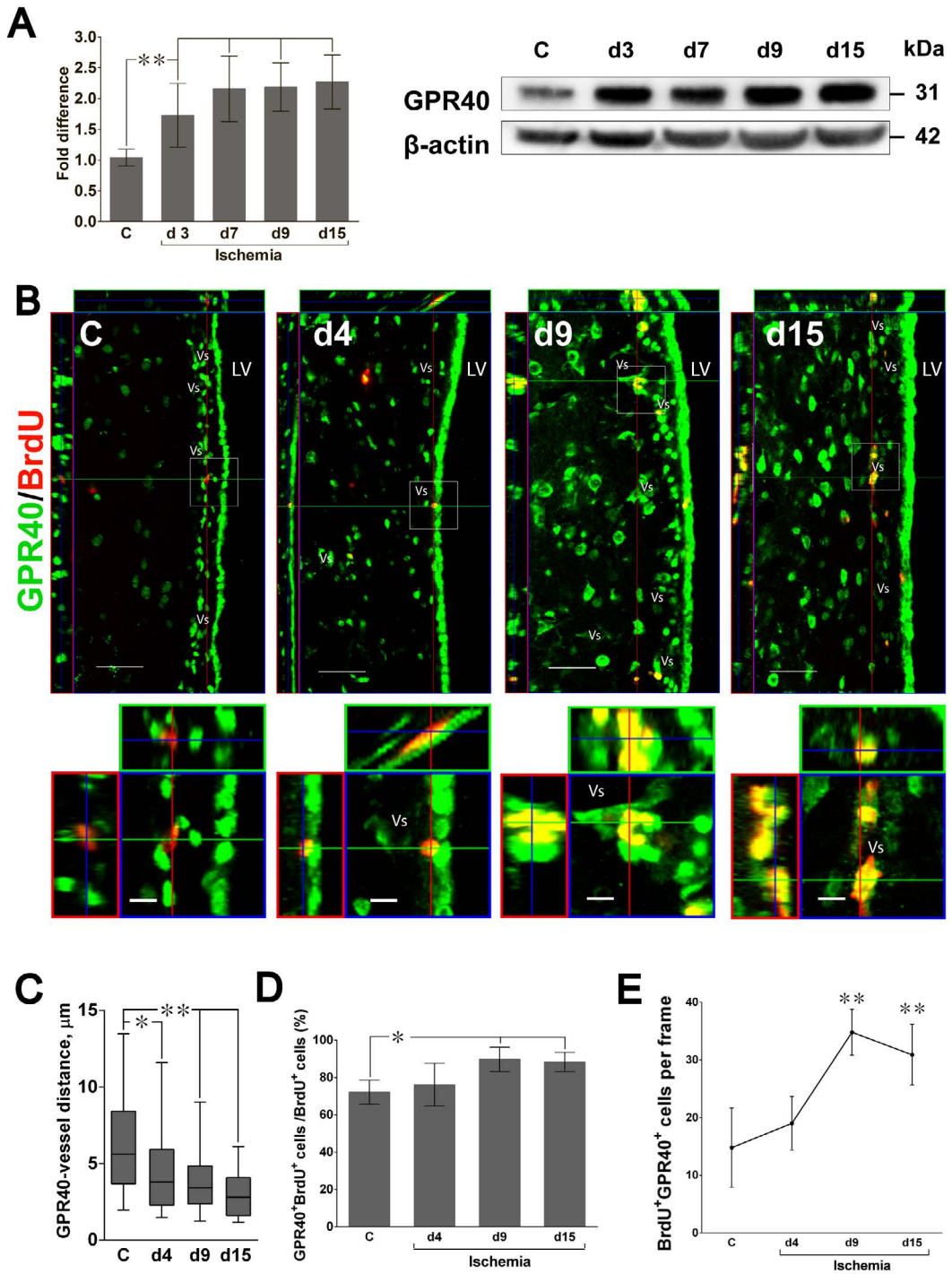

Figure 1: (A) Upregulation of GPR40 in the SVZ after ischemia in monkeys. Equal amounts of the SVZ whole-tissue lysates of the control (C) and post-ischemic days 3 (d3), 7 (d7), 9 (d9) and 15 (d15) were analyzed by Western blot of GPR40 protein, using β-actin as a loading control. The mean levels of GPR40 protein in each time points were compared to the sham-operated control being scored as 1.0. **P<0.01; Mann-Whitney U-test, bars show SD. The figure shows the representative data from three independent Western blots. Inset shows representative Western blot. (B) Double immunostaining for BrdU (red) and GPR40 (green) in the ipsilateral SVZ of the control (C) or post-ischemic day 4 (d4), day 9 (d9) and day 15 (d15). Note an increase of BrdU/GPR40 double staining of proliferating cells on the post-ischemic days 9 and 15 in comparison to the control. Laser confocal microscopy; LV-lateral ventricle; Vs-blood vessel; scale bar, 50 µm and 10 µm for low and high magnification frame, respectively. For panels C-E number of animals, n=3 for each group of the control and post-ischemic days 4, 9, 15, cells were sampled throughout the layers II, III and IV in dorsal, caudate, and anterior aspects of SVZ; P-values show the results of Mann–Whitney U-test, bars show standard deviation. (C) Quantitative evaluation of the relative proximity of the GPR40+ cells to vessels in the SVZ after ischemia. **P<0.01. (D) Incidence of the GPR40/BrdU double-positive cells among the whole BrdU+ cell population in the SVZ of post-ischemic monkeys. *P<0.05. (E) Quantitative evaluation of the number of GPR40/BrdU double-positive cells throughout the SVZ after ischemia. Note a significant increase of the number of BrdU/GPR40 double-positive cells on days 9 and 15 after ischemia comparing to sham-operated control. **P<0.01.

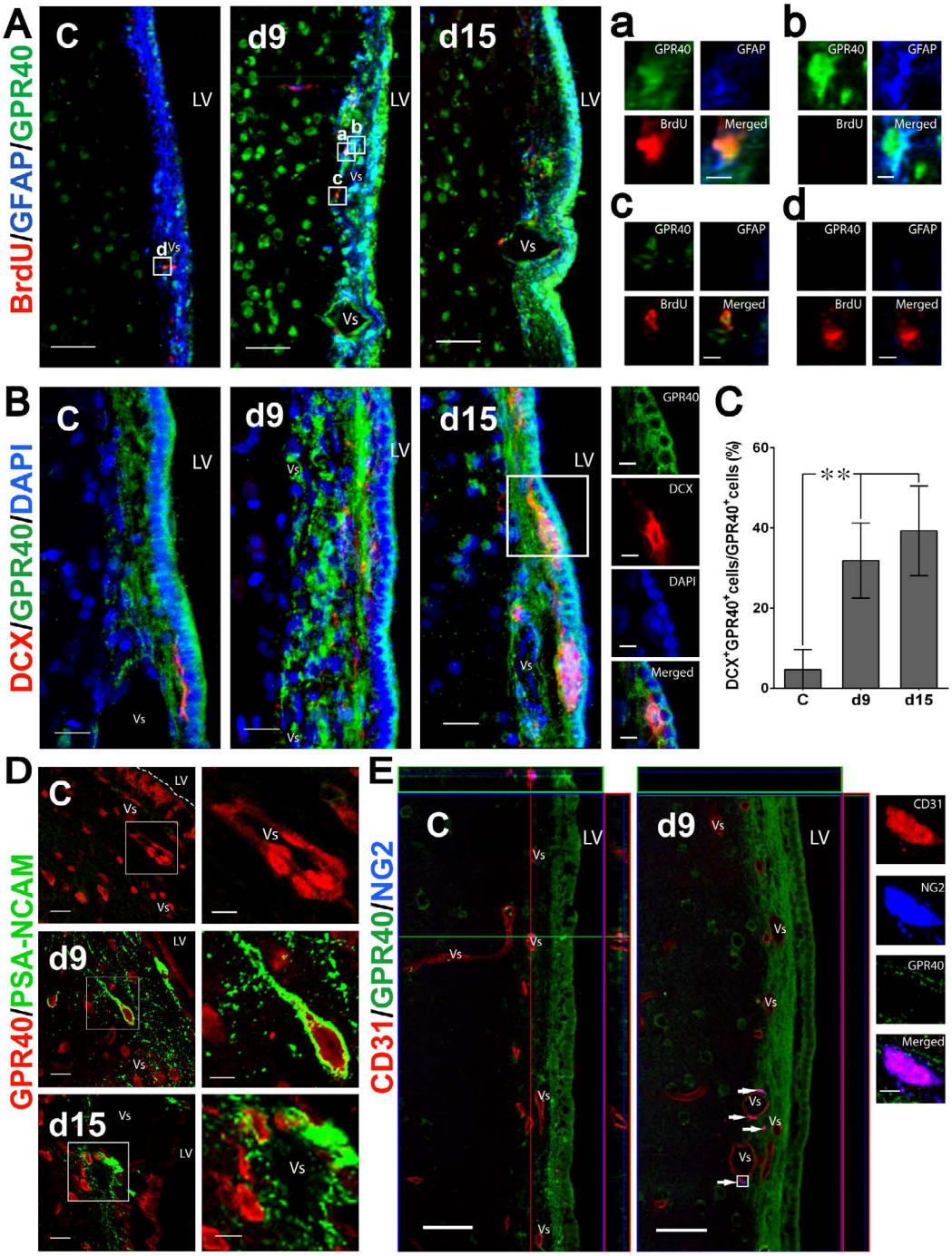

Figure 2: (A). Triple immunostaining for BrdU (red), GFAP (blue) and GPR40 (green) of the control (C) or post-ischemic day 9 (d9) and day 15 (d15) in the SVZ. Note (a) BrdU/GFAP/GPR40 triple-positive neural stem/progenitor cells, (b) GFAP/GPR40 double-positive cells, (c) BrdU/GPR40 double-positive cells and (d) BrdU-positive cells on the post-ischemic day 9. Laser confocal microscopy; scale bar, 50 μm and 5 μm for low and high magnification frame, respectively. For panels A, B, D, E LV-lateral ventricle; Vs-blood vessel. (B) Triple labeling for Dcx (red) GPR40 (green), and DAPI (blue). In the sham-operated control very few Dcx+ cells were detected, while on the post-ischemic days 9 and 15 numerous clusters of Dcx+ immature neurons were revealed in SVZ. Scale bar, 20 μm and 10 μm for 3D reconstruction from low magnification confocal z-series and for high magnification confocal frame, respectively. (C) Incidence of Dcx+ immature neurons among the whole population of GPR40+ cells in the SVZ (number of animals, n=3 for each group of the control and post-ischemic days 9, 15 cells were sampled throughout the layers II, III and IV in dorsal, caudate, and anterior aspects) of the post-ischemic monkeys. Note significant increase of the number of GPR40/Dcx double-positive immature neurons on days 9 and 15 after ischemia. **P<0.01; Mann–Whitney U-test, bars show standard deviation. (D) Expression of GPR40 (red) and PSA-NCAM (green) by the newborn neurons in the SVZ after ischemia. GPR40/PSA-NCAM double-positive cells appear on days 9 and 15. Laser confocal microscopy; LV-lateral ventricle; Vs-blood vessel; scale bar, 20 μm and 10 μm for low and high magnification frame, respectively. (E) Expression of GPR40 in endothelial cells and pericytes in monkey SVZ after ischemia. Triple immunostaining for CD31 (red) GPR40 (green) and NG2 (blue) in the monkey SVZ of the control (C) or post-ischemic day9 (d9). Note the cell which is co-labelled for CD31 and NG2 (high magnification frame). 3D reconstruction from confocal z-series; scale bar, 50 μm and 5 μm for low and high magnification frame, respectively.

progenitor/stem cells during enhanced neurogenesis in the primate SVZ after ischemia.

Perivascular expression of GPR40 in SVZ after ischemia

Concomitant expression of GPR40 with PSA-NCAM was found predominantly in perivascular cells, therefore the cell type of perivascular GPR40-positive cells was studied, using antibodies against CD31 (marker for endothelial cells, macrophages and pericytes) and NG2 (marker for oligodendrocyte precursor cells, macrophages and pericytes). Three-dimensional reconstruction of laser confocal microscopy showed that GPR40+ cells were present near the vessels in SVZ. Some of them were CD31+, but none of GPR40+cells were co-labelled with NG2 (Figure 2E).

Expression of GPR40 by microglial cells in the SVZ vascular niche after ischemia

Microglia were reported to orchestrate both embryonic and adult neurogenesis by regulating the size of the neuronal precursor pool [47,48]. Therefore, the relation of the GPR40-expressing cells with microglia was studied using antibody against microglial marker Iba1. Resting microglial cells are characterized by numerous ramified branching processes, while activated microglia are characterized by a larger soma of amoeboid/rounded macrophage-like shape [20]. Immunofluorescence microscopic analysis revealed Iba1+ microglial cells in layer II (gap) and layer III (astrocytic ribbon) of SVZ to have either ramified or amoeboid phenotypes. The number of Iba1-positive cells in the SVZ significantly increased on day 9 after ischemia (Figures 3A and B). Iba1-positive microglia frequently formed globoid clusters after ischemia near SVZ vessels (Figure 3A). The majority of Iba1+ cells near SVZ vessels co-expressed GPR40 on the second week after ischemia (Figures 3A and C). The co-expression of GPR40 by Iba1+ cells significantly increased on day 9 after ischemia (Figures 3A and C). Moreover, the fraction of GPR40+/Iba1+ cells near SVZ vessels significantly increased on day 9 after ischemia both in total population of SVZ cells and in the cell fraction expressing GPR40 (Figures 3A, D-F). Increase of the number of microglial cells (Figure 3B) and rise of GPR40 expression among microglial cells (Figures 3A and C) occurred simultaneously with migration of immature neurons expressing GPR40 in perivascular regions and in the SVZ gap layer after ischemia (Figures 2B-D). Thus, these data suggest that perivascular GPR40-expressing microglia are conceivably implicated in post-ischemic neurogenesis in adult primate SVZ.

Expression of other signaling molecules implicated in adult neurogenesis in SVZ after ischemia

GPR40 signaling in rodents occurs via Akt, FABP7 and other molecules including stem/progenitor cell markers, as reported previously (Figure 4). Therefore, to evaluate GPR40 implication in those signaling pathways in primate SVZ, correlation of post-ischemic GPR40 protein expression with that of phenotype markers of stem/progenitor cells was studied.

In rodents SHH is known to regulate adult neurogenesis [49] and facilitate ischemia-induced neural progenitor proliferation [34] as well as the proliferation of astrocytes and microglia [50]. Western blot analysis revealed a significant increase of SHH expression in the monkey SVZ on days 3, 7, 9 and 15 after ischemia in comparison to the control (Figures 5A and B). These findings are consistent with our previous data demonstrating increased neurogenesis in monkey SVZ on post-ischemic day 9 [11]. Post-ischemic increase of SHH expression correlated with that of GPR40 (Figure 5C).

Notch1 is indispensable for neurogenesis and maintenance of NSCs in both embryonic and adult brains [51]. Western blot analysis showed a significant increase of Notch1 expression in SVZ on days 3, 7, 9 and 15 after ischemia in comparison to the control (Figures 5A and D). Post-ischemic increase of Notch1 expression correlated with that of both GPR40 and SHH (Figures 5E and F).

β1-integrin, is also required for adult SVZ neurogenesis [52]. Western blot analysis showed a significant increase of β1-integrin expression in SVZ on day 15 after ischemia (Figures 6A and B). Post-ischemic increase of β1-integrin expression correlated with that of GPR40 (Figure 6C).

Sox2 is highly expressed by all SVZ cell types [53] and is critically involved in neural stem cell renewal directly targeting SHH in hippocampal neural precursors in rodents [54]. Western blot analysis demonstrated that Sox 2 expression showed no significant changes on days 3,7 and 9 and significantly decreased on day 15 after ischemia in monkey SVZ (Figures 6A and D).

Expression of GPR40-related signaling molecules in SVZ after ischemia

To investigate spatial relation of GPR40 with other phenotype markers of stem/progenitor cells, co-localization of GPR40 immunoreactivity with that of SHH, Notch1, Sox 2 and β1-integrin was studied in the vascular niche of SVZ after ischemia.

Immunofluorescence microscopic analysis demonstrated moderate or strong co-localization of SHH and GPR40 in microglia with a significant increase of the co-localization (Figure 3F) and increase of the number of microglial cells expressing SHH and GPR40 (Figure 3F) on day 15 after ischemia in SVZ. Moreover, Iba1+ microglia showed a significantly higher SHH expression after ischemia in comparison to the non-microglial cells in SVZ (Figure 3F). Immunofluorescence analysis showed that SHH and GPR40 expression increased predominantly in the vascular niche in the post-ischemic SVZ (Figures 3F and 7A). Post-ischemic increase of the SHH/GPR40 colocalization after ischemia (Figure 3F) is consistent with their correlatively increased expression on Western blot (Figure 5C). FABP7, upstream signalling molecule of GPR40, was also observed on day 15 after ischemia in GPR40+ cells in the SVZ vascular niche (Supplementary Figure S1). Immunofluorescence microscopic analysis showed increase of Notch1 co-expression with GPR40 in the SVZ vascular niche on day 15 after ischemia (Figure 7B). Moreover, co-expression of Notch1 with SHH seen both in control and on day 15 after ischemia was concomitant with post-ischemic increase of SHH and Notch1 immunoreactivity (Figure 7C). Immunofluorescence microscopic analysis demonstrated increase of Sox 2 co-expression with SHH in the SVZ vascular niche on day 9 after ischemia (Figure 7D); as well as GPR40 co-expression with β1-integrin increased on day 9 after ischemia in the SVZ vascular niche (Figure 7E), which is consistent with correlatively increased expression of GPR40 and β1-integrin on Western blot (Figure 6C).

Involvement of GPR40-positive microglia in SHH signaling in SVZ after ischemia

Since SHH and Notch1 appeared to be significantly correlated with the dynamic changes of GPR40 after ischemia (Figures 5C and E), we focused on the related molecules responsible for the GPR40 signaling during post-ischemic neurogenesis. Microglia showed a significantly higher SHH immunoreactivity in the post-ischemic SVZ comparing to non-microglial cells (Figure 3F) and moderate or strong co-localization of SHH with GPR40 increased to mainly strong co-localization after

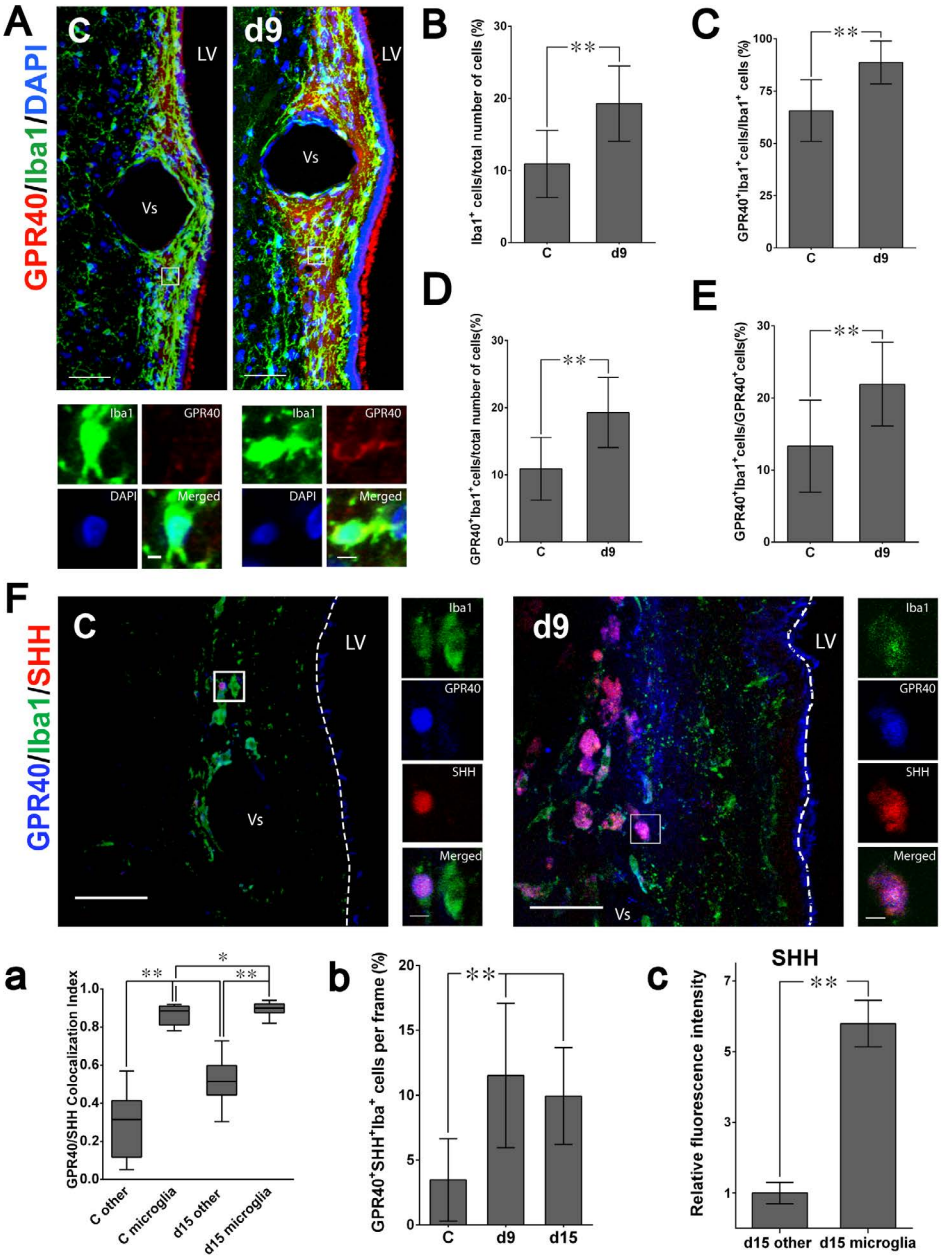

Figure 3: (A) Expression of GPR40 by microglial cells in the SVZ. Triple labeling for GPR40 (red), Iba1 (green) and DAPI (blue) of the control (C) or the post-ischemic day 9 (d9) in the SVZ. Scale bar, 50 μm and 5 μm for the 3D reconstruction from low magnification confocal z-series and for high magnification confocal frame, respectively. For panels A, F LV-lateral ventricle; Vs-blood vessel. For panels B-F number of animals, n=3 for each group of the control and post-ischemic days 9, 15, cells were sampled throughout the layers II, III and IV in dorsal, caudate, and anterior aspects of SVZ. For panels B-F, b, c P-values show the results of Mann–Whitney U-test, bars show standard deviation. **P<0.01. (B) Incidence of Iba1+ cells among all of DAPI-labeled cells in the SVZ of the post-ischemic monkeys. Note a significant increase of the incidence of Iba1-expressive microglial cells on day 9. (C) Incidence of GPR40/Iba1 double-positive cells among all of Iba1+ microglial cells in the SVZ of post-ischemic monkeys. Note significant increase of the fraction of GPR40-expressive microglial cells on day 9. (D) Incidence of GPR40/Iba1 double-positive cells among all of DAPI-labeled cells in SVZ of post-ischemic monkeys. Note a significant increase of the fraction of GPR40-expressive microglial cells on day 9. (E) Incidence of Iba1+ microglia among all of GPR40+ cells in the SVZ of the post-ischemic monkeys. Note a significant increase of the fraction of Iba1+ microglia among all of GPR40-expressive cells on day 9 after ischemia. (F) Expression of GPR40 and SHH by microglial cells in the SVZ in the control (C) or post-ischemic day 9 (d9). Triple immunostaining for GPR40 (blue), Iba1 (green), and SHH (red). Note GPR40/Iba1/SHH triple-positive microglial cells on day 9. 3D reconstruction from confocal z-series; LV-lateral ventricle, scale bar; 50 μm and 5 μm for low and high magnification frame, respectively. (a) Quantitative evaluation of the colocalization between immunoreactivity of GPR40 and SHH in the SVZ of post-ischemic monkeys. The colocalization index is represented by Pearson's coefficient calculated following Costes randomization and unbiased automatic threshold calculation. Pearson's coefficient values within intervals 0-0.49; 0.50-0.70; 0.71-0.88; 0.89-0.97; 0.98-1.0 reveal very weak, weak, moderate, strong and very strong colocalization, respectively. Note moderate or strong GPR40/SHH colocalization in microglia and a significant increase of GPR40/SHH colocalization under ischemia. *P<0.05, **P<0.01. (b) Quantitative evaluation of the number of GPR40/SHH/Iba1 triple-positive cells throughout the SVZ after ischemia. Note a significant increase of the number of GPR40/SHH/Iba1 triple-positive cells on days 9 and 15 after ischemia, in comparison to the sham-operated control. (c) Quantitative evaluation of the relative SHH fluorescence in microglia and other cell types in the SVZ of post-ischemic monkeys. Note significantly higher SHH fluorescence in microglial cells in comparison to other cell types on day 15 after ischemia. Iba1(–) cells are designated "other." The mean of the relative fluorescence intensity for SHH in the Iba1(–) cells was scored as 1.0.

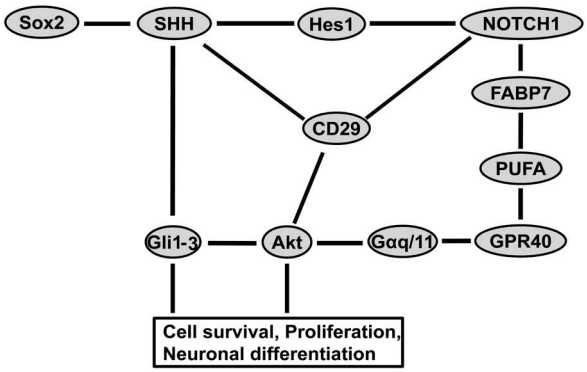

Figure 4: Putative molecular pathways showing how GPR40 is implicated in cell survival, proliferation and differentiation for regulation of adult neurogenesis. The pathways are generated according to the results of the present study and to previous reports, as described in the text.

ischemia (Figure 3F). SHH was predominantly expressed by GPR40-expressing microglia (Figure 3F) and the number of SVZ microglial cells co-expressing SHH and Iba1 increased after ischemia in comparison to the sham-operated control (Figure 3F).

In addition, immunofluorescence microscopic analysis showed that binding of SHH being characterized by its co-localization with Ptc1 in SHH/ Ptc1 complexes occurred in SVZ cells within the distance of SHH paracrine secretion [55] by GPR40+ microglial cells. GPR40+ microglia showed a high SHH expression, while surrounding cells showed negligible intracellular unbound SHH, and mild amounts of SHH co-localized with Ptc1 in a few isolated vesicles (Figure 7F). These data suggest that SHH in SHH/ Ptc1 complexes can originate by paracrine secretion from GPR40+ microglial cells, since presumably they have the highest SHH expression in the adult monkey SVZ.

Discussion

In this study TGBI enhanced proliferation of neuronal precursors and microglial cells in the SVZ along with the increase of perivascular expression of GPR40. GPR40 was expressed in stem/progenitor cells, as well as in the majority of neuronal precursors and microglial cells. Consistent with these findings, the post-ischemic up-regulation of GPR40 occurred in parallel with the increase of SHH and Notch1 expression in the SVZ. Moreover, early increase of GPR40 protein levels in SVZ starting from post-ischemic day 3 suggest GPR40 involvement in the increased neurogenesis from its outset after ischemia. GPR40 spatial distribution revealed a significant increase of its co-localization with SHH and enhancement of co-expression with other stem/progenitor cell markers such as Notch1, Sox 2 and β1-integrin (Figure 4). These observations suggested that GPR40/SHH co-expressing microglia in the vascular niche of primate SVZ can be a paracrine source of SHH that provides signaling for neural progenitor/stem cells for upregulated neurogenesis after ischemia. GPR40 conceivably plays a crucial role in post-ischemic neurogenesis for supporting neurogenic differentiation of stem/progenitor cells in the primate SVZ *via* the cross-talk between microglia and neuronal progenitors in vascular niche.

Here, we compared the SVZ expression profiles both under normal condition and after TGBI to elucidate the role of GPR40 in the activation of SVZ neurogenesis and to identify the cells involved in adult neurogenesis in macaque monkey. TGBI increased perivascular expression of GPR40 with the maximum on day 9, and a significant increase of GPR40 expression was confirmed in the BrdU-positive cells by the immunofluorescence microscopic analysis (Figures 1B-D and E). The majority of proliferative cells was present as cell clusters or individual cells in the perivascular space of arterioles, venules, and capillaries in SVZ (Figure 1B). Consistent with these findings, expression of the newborn neuronal marker PSA-NCAM suggested that the neuronal progenitor cells residing in the perivascular space give rise to young neurons in SVZ. Dcx is selectively expressed in the newborn neurons, but it is not expressed during later neuronal regenerative events such as gliogenesis or regenerative axonal growth [45]. The present data showed that GPR40 was expressed in both PSA-NCAM-positive immature neurons in the gap layer especially in the perivascular space and Dcx-positive immature neurons mainly in the gap layer. Moreover, the number of both GPR40/PSA-NCAM and GPR40/Dcx double-positive immature neurons considerably increased in the SVZ vascular niche on day 15 after ischemia. TGBI enhances endogenous progenitor cell proliferation in the primate SVZ, and this correlated with the increase of GPR40 expression (Figures 2B-D). These data are consistent with our previous results demonstrating that GPR40 is implicated in neurogenesis in hippocampal neurogenic niche [28,30]. It is likely that GPR40 might be closely related to adult neurogenesis in both the SVZ and hippocampus of the post-ischemic monkeys.

Western blot analysis of GPR40 expression in the relation to that of other specific phenotype markers of stem/progenitor cells demonstrated the correlating post-ischemic up-regulation of GPR40, SHH, Notch1 and β1-integrin in the SVZ (Figures 5C, E, F and 6C), which suggested putative interaction of these pathways during post-ischemic neurogenesis in the SVZ. Sox2 is expressed in the proliferating CNS progenitors and is critically involved in their self-renewal [54]. However, Western blot data showed a decreased expression of Sox2, on day 15 after ischemia (Figures 6A and D). This can be explained by the initiation of differentiation of precursor cells in SVZ, because it is well known, that Sox2 is down-regulated during progenitors' final cell cycle during differentiation, when they become post mitotic [56]. It was reported previously that β1-integrin is expressed in the migrating immature neurons and controls formation of cell chains in the rostral migratory stream and mediates cell proliferation in clusters [52]. In this study we demonstrated that GPR40/β1-integrin co-expression increased after ischemia in the SVZ vascular niche, concomitant with the up-regulation of GPR40.

The present data suggests that GPR40 in SVZ is expressed in different cell types including endothelial, ependymal, neuronal progenitors, astrocytes, but the abundance of the GPR40+ cells near the SVZ vessels, was of microglial origin (Figures 3A and F). Intriguingly,

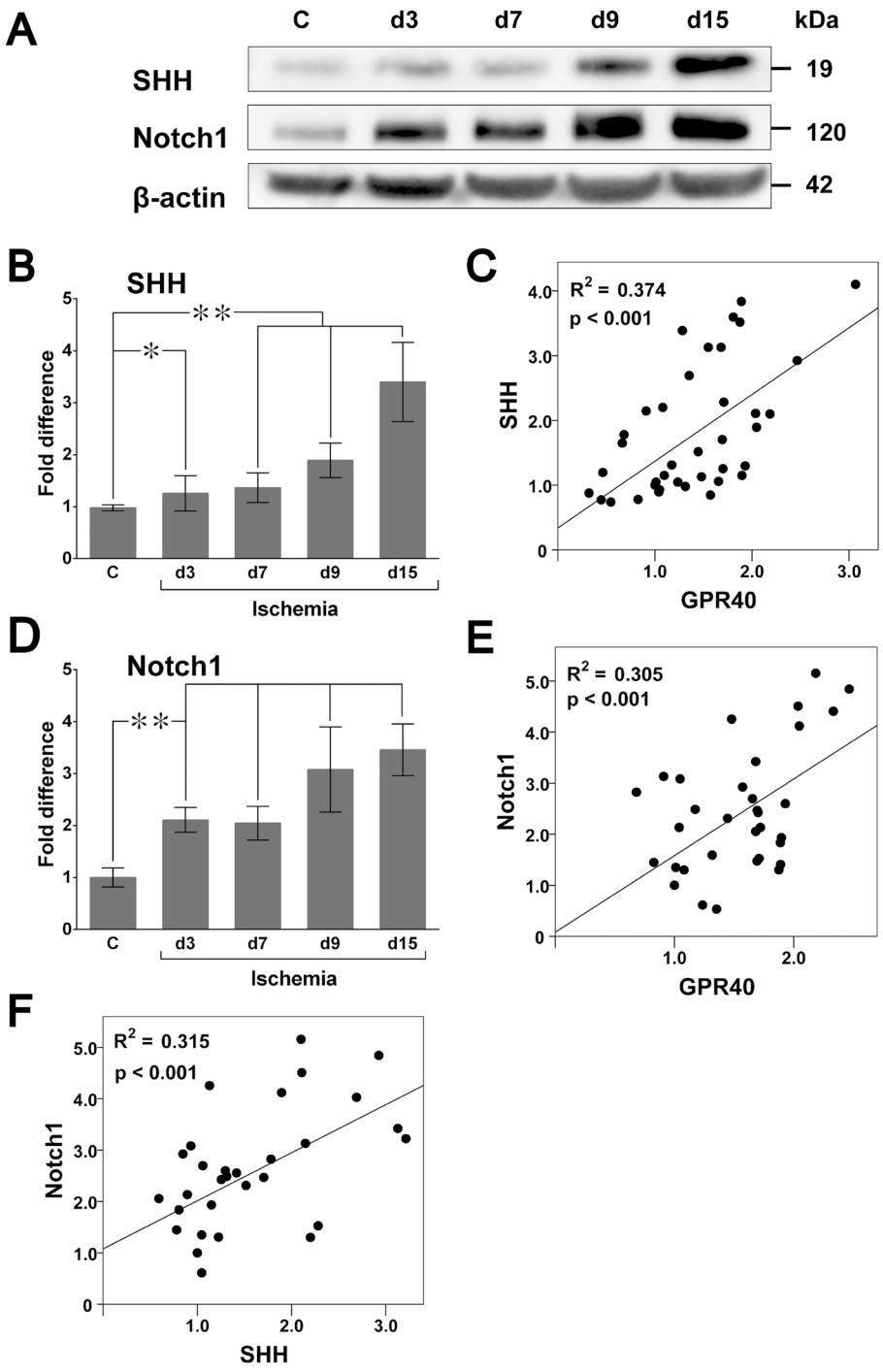

Figure 5: (A) Upregulation of SHH and Notch1 in the monkey SVZ after ischemia. Equal amounts of the SVZ whole-tissue lysates of the control (C) and post-ischemic days 3 (d3), 7 (d7), 9 (d9) and 15 (d15) were analyzed by Western blot of SHH or Notch1 protein, using β-actin as a loading control. The figure shows representative Western blot. For panels B, D the mean levels of SHH and Notch1 protein expression in each time points were compared to the sham-operated control being scored as 1.0. P-values show the results of Mann–Whitney U-test, bars show standard deviation. (B) Western blot densitometry ratios of SHH over β-actin were plotted on the y-axis. Note a significant increase of SHH expression in the monkey SVZ on days 3, 7, 9 and 15 after ischemia. The figure shows the representative data from three independent Western blots. Panels C, E and F show regression analysis of the expression levels of GPR40, SHH and Notch1 in the monkey SVZ after ischemia. Regression lines and coefficients are shown. (C). Western blot densitometry ratios of SHH and GPR40 over β-actin are plotted against each other. Note a significant correlation between the expression of GPR40 and SHH. (D) Western blot densitometry ratios of Notch1 over β-actin were plotted on the y-axis. Note a significant increase of Notch1 expression in the monkey SVZ on days 3, 7, 9 and 15 after ischemia. The figure shows the representative data from three independent Western blots. (E) Western blot densitometry ratios of Notch1 and GPR40 over β-actin are plotted against each other. Note a significant correlation between the expression of GPR40 and Notch1. (F) Western blot densitometry ratios of SHH and Notch1 over β-actin are plotted against each other. Note a significant correlation between the expression of SHH and Notch1.

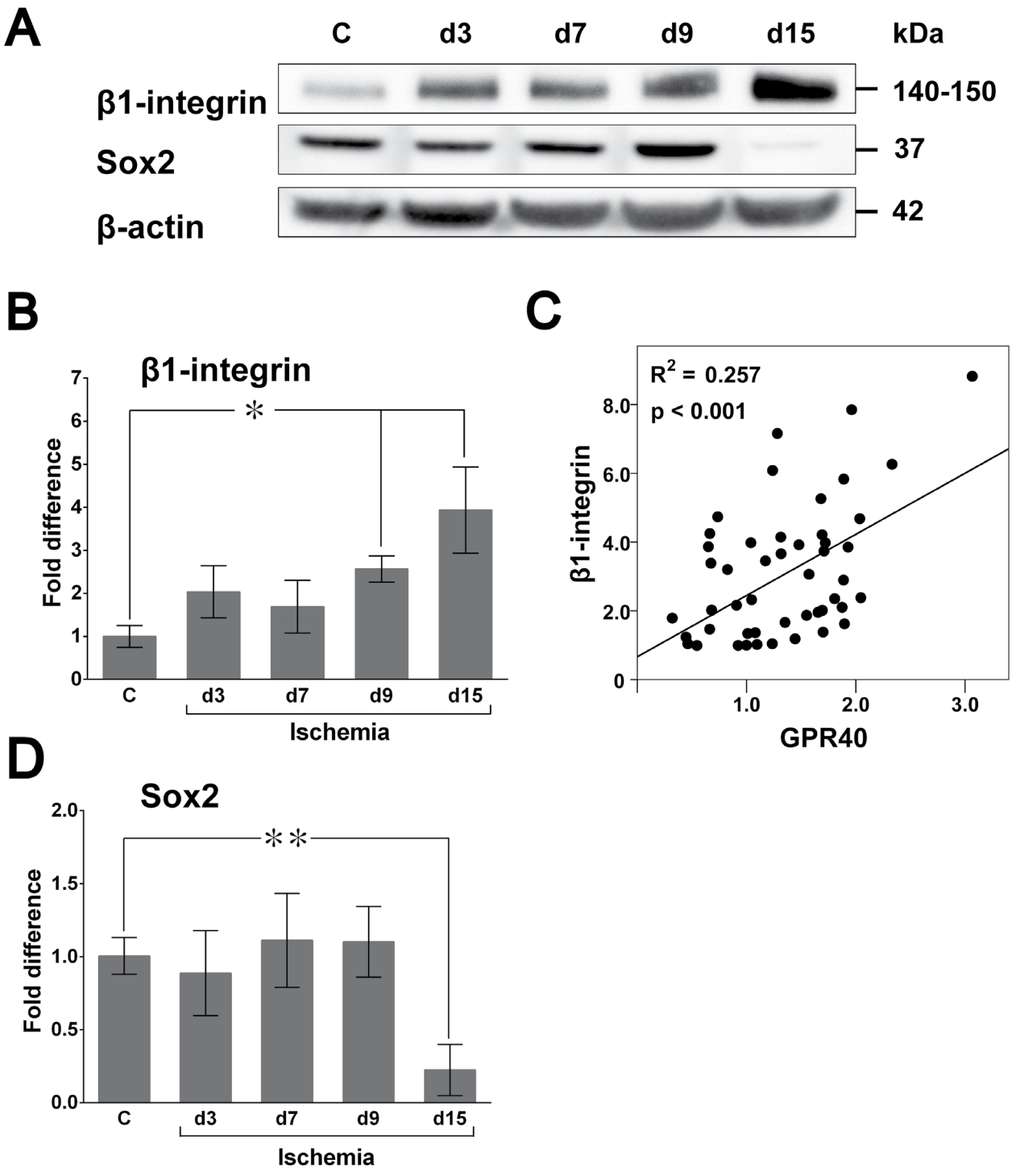

Figure 6: (A) Dynamic changes of β1-integrin and Sox2 protein expression in the monkey SVZ after ischemia. Equal amounts of the SVZ whole-tissue lysates of the control (C) and post-ischemic days 3 (d3), 7 (d7), 9 (d9) and 15 (d15) were analyzed by Western blot of β1-integrin or Sox2 protein, using β-actin as a loading control. The figure shows representative Western blot. For panels B and D the mean levels of β1-integrin or Sox2 protein expression, respectively, in each time points were compared to the sham-operated control being scored as 1.0; P-values show the results of Mann-Whitney U-test, bars show standard deviation. (B) Western blot densitometry ratios of β1-integrin over β-actin were plotted on the y-axis. Note a significant increase of β1-integrin expression in the monkey SVZ on days 9 and 15 after ischemia. *P<0.05. The figure shows the representative data from three independent Western blots. (C) Regression analysis of the expression levels of β1-integrin and GPR40 in the monkey SVZ after ischemia. Western blot densitometry ratios of β1-integrin and GPR40 over β-actin are plotted against each other. Note a significant correlation between the expression of β1-integrin and GPR40. Regression lines and coefficients are shown. (D) Western blot densitometry ratios of Sox2 over β-actin were plotted on the y-axis. Note a significant decrease of Sox2 expression in the monkey SVZ on day 15 after ischemia. **P<0.01. The figure shows the representative data from three independent Western blots.

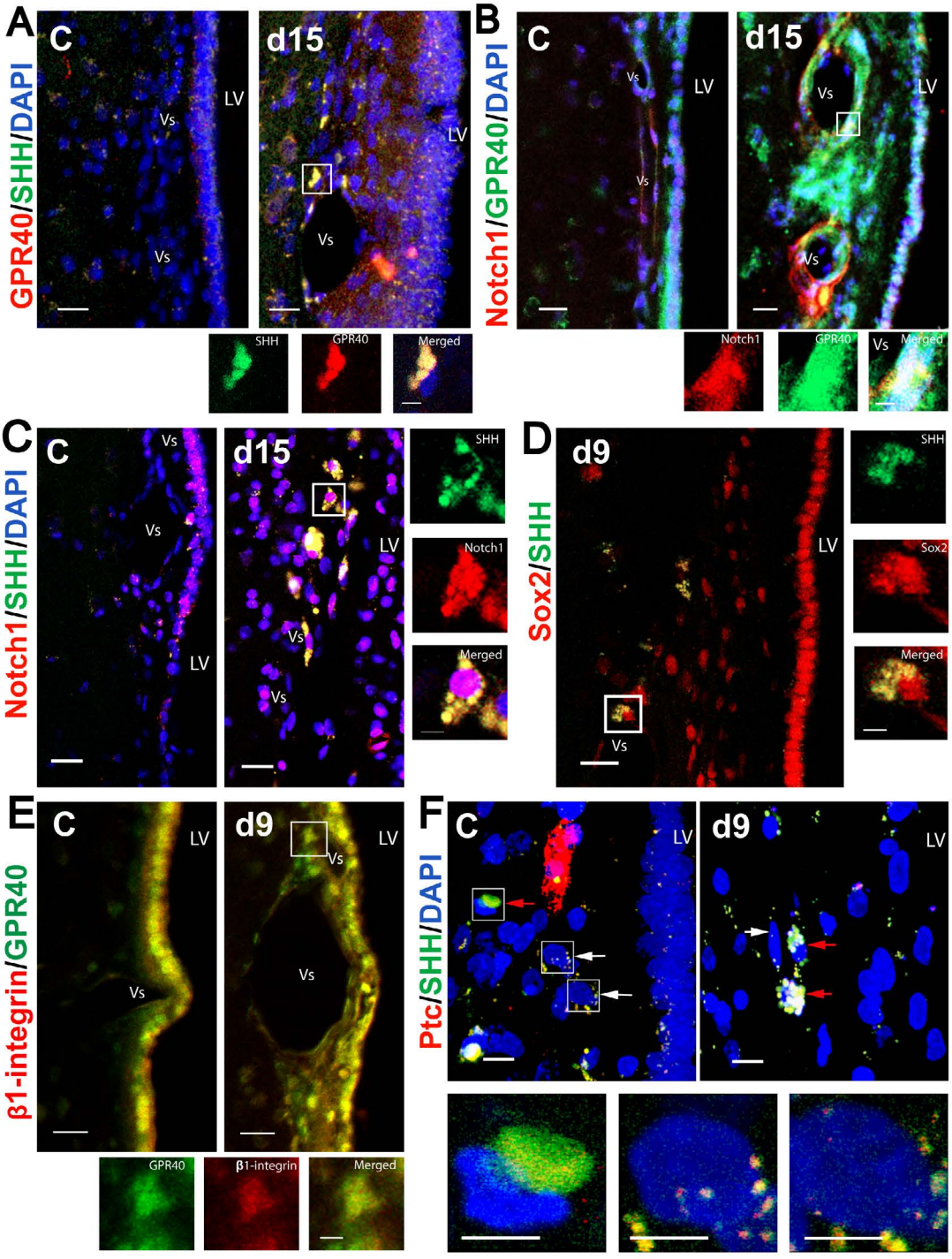

Figure 7: (A) Triple labeling for GPR40 (red), SHH (green), and DAPI (blue) in the monkey SVZ of the control (C) or post-ischemic day 15 (d15). 3D reconstruction from confocal z-series; scale bar, 20 μm. For panels A-F LV-lateral ventricle; Vs-blood vessel. (B) Expression of GPR40 by Notch1+ cells in the monkey SVZ after ischemia. Triple labeling for Notch1 (red), GPR40 (green), and DAPI (blue) in the monkey SVZ of the control (C) or post-ischemic day 15 (d15). Laser confocal microscopy; scale bar, 20 μm and 5 μm for low and high magnification frame, respectively. (C) Triple labeling for Notch1 (red), SHH (green), and DAPI (blue) in the monkey SVZ of the control (C) or post-ischemic day 15 (d15). Laser confocal microscopy; scale bar, 20 μm and 5 μm for low and high magnification frame, respectively. (D) Double immunostaining for Sox2 (red) and SHH (green) in the monkey SVZ of the post-ischemic day 9 (d9). Laser confocal microscopy; scale bar, 50 μm and 5 μm for low and high magnification frame, respectively. (E) Expression of GPR40 by β1-integrin+ cells in the monkey SVZ after ischemia. Double immunostaining for β1-integrin (red) and GPR40 (green) in the monkey SVZ of the control (C) or post-ischemic day 9 (d9). 3D reconstruction from confocal z-series; scale bar, 20 μm and 5 μm for low and high magnification frame, respectively. (F) Triple labeling for Patched (red), SHH (green) and DAPI (blue) in the monkey SVZ of the sham-operated control (C) or post-ischemic day9 (d9). Note GPR40+ cell with high SHH expression (red arrows) and SHH co-localized with Ptc1 in a few isolated vesicles in surrounding cells (white arrows). 3D reconstruction from confocal z-series; scale bar, 10 μm and 5 μm for low and high magnification frame, respectively.

post-ischemic increase of GPR40 expression in SVZ occurred in the area of the gap layer where the increase of the number of microglia of both ramified and rounded/amoeboid cell shape was observed (Figures 3A and F). It is consistent with previous study demonstrating that microglia retain the ability to proliferate in SVZ throughout adulthood and that constitutive activation of microglia is associated with increased proliferation [57]. The present data confirmed most of the Iba1+ cells localized near vessels in the monkey SVZ, to be highly positive for GPR40 (Figures 3A and F). Therefore, we focused on the role of GPR40 in microglia in the SVZ vascular niche.

Expression of SHH by macrophages was reported to orchestrate tumor-associated angiogenesis [58]. Here we found that the SVZ microglial cells express SHH which is essential for the regulation of multipotent stem/progenitor cells in primates. Moreover, GPR40+ microglia express increasing amounts of SHH especially on the second week after ischemia. Although SHH signaling is known to be active in the rodent astrocytes [50,59], most of SHH-expressive cells near the primate SVZ vessels showed a microglial origin (Figure 3F). SHH and Notch pathways are cross-talking feed-forward pathways, since SHH activation feeds forward on the Notch1, *via* the Hes1 in a Notch-ligand independent fashion [60] (Figure 4). Accordingly, we observed the increase of Notch1 expression in the GPR40-expressing cells similar to microglia (Figures 7B and C) as well as the increase of the number of microglial cells expressing SHH in SVZ after ischemia (Figure 3F). Moreover, GPR40 and SHH were co-localized in the GPR40-expressing microglia, and a significant increase of their co-localization was demonstrated by Costes algorithm [43] after ischemia in comparison to the sham-operated monkeys (Figure 3F). It is consistent with correlative changes in the expression of GPR40 with both SHH and Notch1 in SVZ after ischemia (Figures 5C, E and F). These data suggest that GPR40 is involved in SHH and Notch1 signaling, and that the GPR40+ microglia could be implicated in the SHH and Notch1 signaling to regulate neurogenic divisions of SVZ progenitors after ischemia.

In different tissues, SHH signaling was reported to involve a) its paracrine secretion by SHH-producing cells, b) transport over considerable distances, c) consequent binding to Ptc1 receptors on the surface of SHH responding cells and internalization of Ptc1/SHH complexes into endosomes [35] and d) their targeting for protein degradation [36] with half-life less than one hour [37]. According to our data for the SHH immunoreactivity (Figure 3F), the main candidate for the paracrine secretion of SHH in the monkey SVZ is GPR40/SHH-expressing microglia, because it showed the highest expression of SHH relative to all other cell types in the SVZ. We speculate that high expression of SHH in the GPR40+ microglia after ischemia induces secretion of SHH, which should be implicated in post-ischemic neurogenesis in the monkey SVZ. Receptor-mediated endocytosis of SHH is an inherent activity of Ptc1, and SHH internalization is a characteristic feature of signaling in the neural plate cells [35]. When Ptc1 targets SHH to endocytosis, internalized SHH is degraded in the receiving cells [36] with half-life less than one hour [37]. In this study, binding of SHH with formation Ptc1/SHH complexes was confirmed to occur in the cells that surrounded GPR40/SHH-expressing microglia. However, the immunofluorescence microscopic analysis demonstrated that immunoreactivity of intracellular unbound SHH in the cells that surrounded GPR40/SHH-expressing microglia remained negligible both in the control and after ischemia (Figure 7F). This suggests extracellular origin of SHH conjugated with Ptc1 in the cells of non-microglial morphology in the SVZ vascular niche. Presumably, GPR40/SHH-expressing microglia in the vascular niche of primate SVZ serve as a source of paracrine secretion of SHH and provide orchestrating signaling for neural progenitor/stem cells during neurogenesis after ischemia.

Conclusion

Based on the present data, we speculate that, 1) in the SVZ vascular niche SHH in non-microglial cells is mainly of extracellular origin; 2) the main candidate for paracrine secretion of SHH in monkey SVZ is GPR40/SHH-expressing microglia; and 3) GPR40 is implicated in post-ischemic neurogenesis in the adult primate SVZ via the cross-talk between microglia and neuronal progenitors in the vascular niche by involving SHH and Notch1 signaling (Figure 4). Thus, the present data provide a basis for clarifying the role of GPR40 in SVZ neurogenesis in adult primates.

Acknowledgement

This study was supported by the grants Kiban-Kennkyu (B) (18390392, 22390273) from the Japanese Ministry of Education, Culture, Sports, Science and Technology. The support of Grant DN13/10/2017 of the National Science Fund of Bulgaria is also acknowledged.

References

1. Altman J (1962) Are new neurons formed in the brains of adult mammals? Science 135: 1127-1128.
2. Eriksson PS, Perfilieva E, Björk-Eriksson T, Alborn AM, Nordborg C, et al. (1998) Neurogenesis in the adult human hippocampus. Nat Med 4: 1313-1317.
3. Sawamoto K, Wichterle H, Gonzalez-Perez O, Cholfin JA, Yamada M, et al. (2006) New neurons follow the flow of cerebrospinal fluid in the adult brain. Science 311: 629-632.
4. Leuner B, Mendolia-Loffredo S, Kozorovitskiy Y, Samburg D, Gould E, et al. (2004) Learning enhances the survival of new neurons beyond the time when the hippocampus is required for memory. J Neurosci 24: 7477-7481.
5. Aimone JB, Wiles J, Gage FH (2006) Potential role for adult neurogenesis in the encoding of time in new memories. Nat Neurosci 9: 723-727.
6. Gage FH (2000) Mammalian neural stem cells. Science 287: 1433-1438.
7. Quiñones-Hinojosa A, Sanai N, Soriano-Navarro M, Gonzalez-Perez O, Mirzadeh Z, et al. (2006) Cellular composition and cytoarchitecture of the adult human subventricular zone: a niche of neural stem cells. J Comp Neurol 494: 415-434.
8. Sanai N, Tramontin AD, Quiñones-Hinojosa A, Barbaro NM, Gupta N, et al. (2004) Unique astrocyte ribbon in adult human brain contains neural stem cells but lacks chain migration. Nature 427: 740-744.
9. Doetsch F, Caillé I, Lim DA, García-Verdugo JM, Alvarez-Buylla A (1999) Subventricular zone astrocytes are neural stem cells in the adult mammalian brain. Cell 97: 703-716.
10. Gould E, Tanapat P, McEwen BS, Flügge G, Fuchs E (1998) Proliferation of granule cell precursors in the dentate gyrus of adult monkeys is diminished by stress. Proc Natl Acad Sci USA 95: 3168-3171.
11. Tonchev AB, Yamashima T, Sawamoto K, Okano H (2005) Enhanced proliferation of progenitor cells in the subventricular zone and limited neuronal production in the striatum and neocortex of adult macaque monkeys after global cerebral ischemia. J Neurosci Res 81: 776-788.
12. Shen Q, Wang Y, Kokovay E, Lin G, Chuang SM, et al. (2008) Adult SVZ stem cells lie in a vascular niche: A quantitative analysis of niche cell-cell interactions. Cell Stem Cell 3: 289-300.
13. Tavazoie M, Van der Veken L, Silva-Vargas V, Louissaint M, Colonna L, et al. (2008) A specialized vascular niche for adult neural stem cells. Cell Stem Cell 3: 279-288.
14. Yamashima T, Tonchev AB, Vachkov IH, Popivanova BK, Seki T, et al. (2004) Vascular adventitia generates neuronal progenitors in the monkey hippocampus after ischemia. Hippocampus 14: 861-875.
15. Alvarez-Buylla A, Lim DA (2004) For the long run: Maintaining germinal niches in the adult brain. Neuron 41: 683-686.
16. Walton NM, Sutter BM, Laywell ED, Levkoff LH, Kearns SM, et al. (2006) Microglia instruct subventricular zone neurogenesis. Glia 54: 815-825.
17. Mercier F, Kitasako JT, Hatton GI (2002) Anatomy of the brain neurogenic zones revisited: fractones and the fibroblast/macrophage network. J Comp Neurol 451: 170-188.

18. Butovsky O, Ziv Y, Schwartz A, Landa G, Talpalar AE, et al. (2006) Microglia activated by IL-4 or IFN-gamma differentially induce neurogenesis and oligodendrogenesis from adult stem/progenitor cells. Mol Cell Neurosci 31: 149-160.

19. Ueno M, Yamashita T (2014) Bidirectional tuning of microglia in the developing brain: From neurogenesis to neural circuit formation. Curr Opin Neurobiol 27: 8-15.

20. Mosher KI, Andres RH, Fukuhara T, Bieri G, Hasegawa-Moriyama M, et al. (2012) Neural progenitor cells regulate microglia functions and activity. Nat Neurosci 15: 1485-1487.

21. Iwai M, Sato K, Kamada H, Omori N, Nagano I, et al. (2003) Temporal profile of stem cell division, migration, and differentiation from subventricular zone to olfactory bulb after transient forebrain ischemia in gerbils. J Cereb Blood Flow Metab 23: 331-341.

22. Sawzdargo M, George SR, Nguyen T, Xu S, Kolakowski LF, et al., (1997) A cluster of four novel human G protein-coupled receptor genes occurring in close proximity to CD22 gene on chromosome 19q13.1. Biochem Biophys Res Commun 239: 543-547.

23. Itoh Y, Kawamata Y, Harada M, Kobayashi M, Fujii R, et al. (2003) Free fatty acids regulate insulin secretion from pancreatic beta cells through GPR40. Nature 422: 173-176.

24. Briscoe CP, Tadayyon M, Andrews JL, Benson WG, Chambers JK, et al. (2003) The orphan G protein-coupled receptor GPR40 is activated by medium and long chain fatty acids. J Biol Chem 278: 11303-11311.

25. Ma D, Tao B, Warashina S, Kotani S, Lu L, et al. (2007) Expression of free fatty acid receptor GPR40 in the central nervous system of adult monkeys. Neurosci Res 58: 394-401.

26. Sartorius T, Drescher A, Panse M, Lastovicka P, Peter A, et al., (2015) Mice Lacking Free Fatty Acid Receptor 1 (GPR40/FFAR1) are Protected Against Conjugated Linoleic Acid-Induced Fatty Liver but Develop Inflammation and Insulin Resistance in the Brain. Cell Physiol Biochem 35: 2272-2284.

27. Boneva NB, Kaplamadzhiev DB, Sahara S, Kikuchi H, Pyko IV, et al. (2011) Expression of fatty acid-binding proteins in adult hippocampal neurogenic niche of postischemic monkeys. Hippocampus 21: 162-171.

28. Yamashima T (2012) 'PUFA-GPR40-CREB signaling' hypothesis for the adult primate neurogenesis. Prog Lipid Res 51: 221-231.

29. Yamashima T (2015) Dual effects of the non-esterified fatty acid receptor 'GPR40' for human health. Prog Lipid Res 58: 40-50.

30. Ma D, Lu L, Boneva NB, Warashina S, Kaplamadzhiev DB, et al. (2008) Expression of free fatty acid receptor GPR40 in the neurogenic niche of adult monkey hippocampus. Hippocampus 18: 326-333.

31. Boneva NB, Yamashima T (2012) New insights into "GPR40-CREB interaction in adult neurogenesis" specific for primates. Hippocampus 22: 896-905.

32. Mathivanan A, Minabe Y, Ota T, Nagata N, Shima KR, et al. (2016) Role of GPR40 for fish oil PUFA-mediated BDNF Synthesis in the Monkey Hippocampus. J Alzheimers Dis Parkinsonism 6: 213.

33. Tsukada H, Kakiuchi T, Fukumoto D, Nishiyama S, Koga K (2000) Docosahexaenoic acid (DHA) improves the age-related impairment of the coupling mechanism between neuronal activation and functional cerebral blood flow response: A PET study in conscious monkeys. Brain Res 862: 180-186.

34. Sims JR, Lee SW, Topalkara K, Qiu J, Xu J, et al. (2009) Sonic hedgehog regulates ischemia/hypoxia-induced neural progenitor proliferation. Stroke 40: 3618-3626.

35. Incardona JP, Lee JH, Robertson CP, Enga K, Kapur RP, et al. (2000) Receptor-mediated endocytosis of soluble and membrane-tethered Sonic hedgehog by Patched-1. Proc Natl Acad Sci USA 97: 12044-12049.

36. Torroja C, Gorfinkiel N, Guerrero I (2004) Patched controls the Hedgehog gradient by endocytosis in a dynamin-dependent manner, but this internalization does not play a major role in signal transduction. Development 131: 2395-2408.

37. Guy RK (2000) Inhibition of sonic hedgehog autoprocessing in cultured mammalian cells by sterol deprivation. Proc Natl Acad Sci USA 97: 7307-7312.

38. Yamashima T, Saido TC, Takita M, Miyazawa A, Yamano J, et al. (1996) Transient brain ischaemia provokes Ca2+, PIP2 and calpain responses prior to delayed neuronal death in monkeys. Eur J Neurosci 8: 1932-1944.

39. Yamashima T, Kohda Y, Tsuchiya K, Ueno T, Yamashita J, et al. (1998) Inhibition of ischaemic hippocampal neuronal death in primates with cathepsin B inhibitor CA-074: A novel strategy for neuroprotection based on 'calpain-cathepsin hypothesis'. Eur J Neurosci 10: 1723-1733.

40. Kuhn HG, Dickinson-Anson H, Gage FH (1996) Neurogenesis in the dentate gyrus of the adult rat: Age-related decrease of neuronal progenitor proliferation. J Neurosci 16: 2027-2033.

41. Arribas SM, Daly CJ, McGrath IC (1999) Measurements of vascular remodeling by confocal microscopy. Methods Enzymol 307: 246-273.

42. Bolte S, Cordelières FP (2006) A guided tour into subcellular colocalization analysis in light microscopy. J Microsc 224: 213-232.

43. Costes SV, Daelemans D, Cho EH, Dobbin Z, Pavlakis G, et al. (2004) Automatic and quantitative measurement of protein-protein colocalization in live cells. Biophys J 86: 3993-4003.

44. Zinchuk V, Wu Y, Grossenbacher-Zinchuk O (2013) Bridging the gap between qualitative and quantitative colocalization results in fluorescence microscopy studies. Sci Rep 3: 1365.

45. Couillard-Despres S, Winner B, Schaubeck S, Aigner R, Vroemen M, et al. (2005) Doublecortin expression levels in adult brain reflect neurogenesis. Eur J Neurosci 21: 1-14.

46. Doetsch F, Garcia-Verdugo JM, Alvarez-Buylla A (1997) Cellular composition and three-dimensional organization of the subventricular germinal zone in the adult mammalian brain. J Neurosci 17: 5046-5061.

47. Cunningham CL, Martínez-Cerdeño V, Noctor SC (2013) Microglia regulate the number of neural precursor cells in the developing cerebral cortex. J Neurosci 33: 4216-4233.

48. Sierra A, Encinas JM, Deudero JJ, Chancey JH, Enikolopov G, et al. (2010) Microglia shape adult hippocampal neurogenesis through apoptosis-coupled phagocytosis. Cell Stem Cell 7: 483-495.

49. Lai K, Kaspar BK, Gage FH, Schaffer DV (2003) Sonic hedgehog regulates adult neural progenitor proliferation in vitro and in vivo. Nat Neurosci 6: 21-27.

50. Pitter KL, Tamagno I, Feng X, Ghosal K, Amankulor N, et al. (2014) The SHH/Gli pathway is reactivated in reactive glia and drives proliferation in response to neurodegeneration-induced lesions. Glia 62: 1595-1607.

51. Imayoshi I, Sakamoto M, Yamaguchi M, Mori K, Kageyama R (2010) Essential roles of Notch signaling in maintenance of neural stem cells in developing and adult brains. J Neurosci 30: 3489-3498.

52. Belvindrah R, Hankel S, Walker J, Patton BL, Müller U (2007) Beta1 integrins control the formation of cell chains in the adult rostral migratory stream. J Neurosci 27: 2704-2717.

53. Lim DA, Alvarez-Buylla A (2014) Adult neural stem cells stake their ground. Trends Neurosci 37: 563-571.

54. Favaro R, Valotta M, Ferri AL, Latorre E, Mariani J, et al. (2009) Hippocampal development and neural stem cell maintenance require Sox2-dependent regulation of Shh. Nat Neurosci 12: 1248-1256.

55. Ruiz i Altaba A, Palma V, Dahmane N (2002) Hedgehog-Gli signalling and the growth of the brain. Nat Rev Neurosci 3: 24-33.

56. Graham V, Khudyakov J, Ellis P, Pevny L (2003) SOX2 functions to maintain neural progenitor identity. Neuron 39: 749-765.

57. Butovsky O, Landa G, Kunis G, Ziv Y, Avidan H, et al., (2006) Induction and blockage of oligodendrogenesis by differently activated microglia in an animal model of multiple sclerosis. J Clin Invest 116: 905-915.

58. Valverde Lde F, Pereira Tde A, Dias RB, Guimarães VS, Ramos EA, et al. (2016) Macrophages and endothelial cells orchestrate tumor-associated angiogenesis in oral cancer via hedgehog pathway activation. Tumour Biol 37: 9233-9241.

59. Amankulor NM, Hambardzumyan D, Pyonteck SM, Becher OJ, Joyce JA, et al. (2009) Sonic hedgehog pathway activation is induced by acute brain injury and regulated by injury-related inflammation. J Neurosci 29: 10299-10308.

60. Ingram WJ, McCue KI, Tran TH, Hallahan AR, Wainwright BJ (2008) Sonic Hedgehog regulates Hes1 through a novel mechanism that is independent of canonical Notch pathway signalling. Oncogene 27: 1489-1500.